Theoretical Chemistry Accounts (2024) 143:8
https://doi.org/10.1007/s00214-023-03081-x

REGULAR ARTICLE

Enthalpy of formation of sodium, magnesium and lithium compounds with composite methods

Cleuton de Souza Silva[1]

Received: 27 October 2021 / Accepted: 30 November 2023 / Published online: 27 December 2023

Abstract

The heats of formation of forty-six molecules containing sodium, lithium and magnesium atoms have been calculated using G3X-CEP, G3X(CCSD)-CEP, G4, EnAt1, EnAt2, G3B3, G3MP2B3, CBS-QB3 and functionals using the atomization. The discrepancies between the predicted and the reported heats of formation vary in the range of 0.0–85 kcal mol^{-1}. The best agreement with experimental data was achieved by using Gn and Gn-CEP multilevel techniques. It was found that the best performance among density functional theory (DFT) methods within the atomization approach demonstrated the long range corrected LC-wPBE and BMK level theory. Composite methods presented the best results when compared with DFT. The G4, which was recently reported as a very accurate method for calculating enthalpies of formation, presented the best results when compared with DFT and other composite methods.

Keywords Sodium compounds · Lithium compounds · Magnesium compounds · EnAt1 · EnAt2 · Composite methods

1 Introduction

In its metallic form, sodium is fundamental in the production of esters [1] and in the generation of organic compounds. Sodium is also a component of sodium chloride, which is an extremely important compound found throughout the environment. Other applications are: upgrading the structure of alloys [2], sodium vapour lamps, descaling metals and purifying molten metals [3].

Sodium is a very reactive element; it oxidises quickly in contact with humid air. If exposed to light, it combines with chlorine to form sodium chloride. To obtain pure sodium, the electrolysis of molten sodium hydroxide is used. This electrolysis cannot be carried out in an aqueous medium, as sodium reacts immediately with water to form sodium hydroxide. Sodium has a solid physical state, body-centred cubic crystal structure, with colour and silvery-white appearance.

Lithium is found in rechargeable batteries [4], which are used for laptops, mobile phones and electric vehicles. Lithium is also used in every non-rechargeable battery for heart pacemakers, toys and clocks. Lithium metal is converted into alloys with aluminium and magnesium [5], upgrading their strength and making them lighter. A magnesium-lithium alloy is employed for reinforcement plating, whilst aluminium–lithium alloys [6] are employed in aircraft, bicycle frames and high-speed trains.

Lithium, in its metallic form, has a greyish-white colour. Among all the metals in the Periodic Table, it has the lowest density value. Another reaction characteristic that lithium has in common with alkali metals is the reaction with halogens and hydrogen gas when heated. Only lithium can react with nitrogen gas to form lithium nitride, Li_3N, at room temperature.

Magnesium is the lightest of all metals used as the basis for constructional alloys [7]. It is this property that entices automobile manufacturers to replace denser materials, not only steels, cast irons and copper-based alloys but even aluminium alloys, with magnesium-based alloys. Because of its similarities with aluminium, magnesium can be used as a substitute for many, if not most, aluminium applications [7]. However, magnesium is still limited by its extractions costs.

Magnesium is a very active metal. It reacts slowly with cold water and more quickly with hot water. It is not found

SI in honour of Prof. Ramon Carbó-Dorca Dr. Tanmoy Chakraborty.

✉ Cleuton de Souza Silva
cleutonsouza@ufam.edu.br

[1] Instituto de Ciências Exatas e Tecnologia, Universidade Federal do Amazonas, Campus de Itacoatiara, Itacoatiara, AM 69100-021, Brazil

free in its native state but in the form of compounds. Magnesium is a low-density solid at ambient conditions and is silvery-white in colour. When burned, magnesium oxide is formed through a synthesis or addition reaction with oxygen present in the air. Magnesium metal can be mixed with other metals to form metal alloys.

The enthalpy of formation (298.15 K) of compounds of sodium, magnesium and lithium, calculated with composite methods, presented better results when compared with ab initio methods. Vasiliu et al. [8, 9] showed (CCSD(T)/aug-cc-pwCVnZ) geometry parameters, frequencies, heats of formation, and bond energies are found to be in good agreement with reliable experimental results for compounds of sodium, magnesium and lithium.

Curtiss et al. [10, 11] calculated that LiNa presented a deviation of 0.58 kcal mol^{-1} for G4; whereas, for the density functional theory (DFT) with 6–311 + G(3df,2p), the deviation was 2.9, − 4.1 and 3.9 kcal mol^{-1} for B97-2 [10], B1B95 [10] and VSXC [10], respectively.

A meaningful improvement in reducing computational costs while ensuring the accuracy of the calculations has been newly developed by Pereira et al. [12], which associates a compact effective potential (CEP) [13] with the G3 theory, resulting in a method known as G3CEP [12]. Other proposals were then expanded, such as G4-CEP [14], G3X-CEP [15] and G3X(CCSD)-CEP [15], using this prosperous generalization and combining pseudopotential with the G3 theory [15]. Utilization of these composite methods demonstrates a significant decrease in CPU time, conserving outstanding accuracy when compared with the original Gn versions. These methods were applied to transition metals [16], pKa [17, 18], and Enthalpies of formation of compounds of aluminium [19], for example.

Recently, the G3X(CCSD) and G3X composite methods have been gathered with pseudopotential. Silva and Custodio [15] publicise the opportunity to improve the calculated heats of formation with respect to accurate experimental data by scaling the atomization energies. This series of steps, along with the G3X and G3X(CCSD) methods and pseudopotential, creates EnAt1 [15] and EnAt2 [15], which provide results that are as accurate as the combination of G4CEP [14] and G3CEP [12] theories.

For heats of formation from the G3/05 test set, Silva and Custodio showed that the MAD of the calculations with EnAt1 (1.0 kcal mol^{-1}) and EnAt2 (1.0 kcal mol^{-1}) are better than G3X-CEP (1.2 kcal mol^{-1}) and G3X(CCSD)-CEP (1.1 kcal mol^{-1}) with the original experimental atomization energies. They also calculated that Na_2 showed a deviation of 2.1 and 2.1 kcal mol^{-1} for G3X-CEP and G3X(CCSD)-CEP, respectively, whereas the MAD for the EnAt1 and EnAt2 methods was 0.0 and -0.4 kcal mol^{-1}, respectively.

The objective of this work was to determine the thermochemical values of compounds of sodium, magnesium and lithium using the EnAt1 and EnAt2 methods in order to establish which presented the best results.

1.1 Computational methods

The enthalpies of formation at 298.15 K were predicted from the total atomization energies. This needs an appropriate and balanced energetic account of the molecule and its constituent atoms, which places rigorous requirements on the quantum methods used.

The results obtained atomization using the density functional theory (DFT) with different exchange and correlation: B2PLYP [20], BMK [21], M06 [22], M06-HF [22], LC-wPBE [23, 24], PBE0 [24, 25], wB97XD [26], O3LYP [27] and mPW1PW91 [28]. The 6-311G(d,p) [29, 30], aug-cc-pVDZ [31, 32] and aug-cc-pVTZ [31, 32] basis sets were employed in the DFT. Besides the optimized geometries at the B3LYP/6-311G(d,p) level, different strategies have been adopted by the composite methods, such as the following:

i. B3LYP/6-311G(d,p) was used by B2PLYP, BMK, M06, M06-HF, LC-wPBE, PBE0, wB97XD and O3LYP for the geometry optimization with a scaling factor of $\lambda = 0.99$ for vibrational frequencies;
ii. B3LYP/6-31G(2df,p) was used by G3X-CEP, G3X(CCSD)-CEP, G4, EnAt1 and EnAt2 for geometry optimization and frequencies with $\lambda = 0.9854$;
iii. B3LYP/6-31G(d) was used by G3B3 [33] and G3MP2B3 [33] for geometry optimization and frequencies with $\lambda = 0.960$;
iv. B3LYP/6-311G(2d,d,p) was used by CBS-QB3 [34] for geometry optimization and frequencies with $\lambda = 0.99$;
v. Extrapolation(1) and Extrapolation(2) are described in G4 theory [11]. In summary, the energy limit E_{limit} is calculated. The basis set limit is determined using two-point extrapolation and Dunning's aug-cc-pVnZ basis sets:
$$E_{aug\text{-}cc\text{-}pVnZ} = [E_{n+1} - E_n \quad exp(-1.63)] \; / \; [1 - exp(-1.63)]$$
Where:
aug-cc-pVDZ and aug-cc-pVTZ extrapolation(1)
aug-cc-pVTZ and aug-cc-pVQZ extrapolation(2)
vi. Extrapolation(3) and extrapolation(4) are described in the paper by chinini and custodio [35],
$$e(n) = ECBS + A(n + \xi)^{-3b}$$
where:
aug-cc-pVDZ and aug-cc-pVTZ Extrapolation(3)
aug-cc-pVTZ and aug-cc-pVQZ Extrapolation(4)
where E(n) is the energy calculated using an n-zeta basis set and ξ and b are parameters to be optimized with respect to a reference set of calculations. For

B2PLYP, M06, M06-HF, LC-wPBE, PBE0, wB97XD, O3LYP and mPW1PW91, $b = 1.048$ and $\xi = 0.015$; for BMK, $b = 1.271$ and $\xi = -0.039$.

G3X-CEP and G3X(CCSD)-CEP [20] emerge from the junction of the G3X and G3X(CCSD) methods with the CEP pseudopotential. In this case, the G3X reference energy is calculated at the QCISD(T)/6-31G(d) level, for as much as the G3X(CCSD) regards the CCSD(T)/6-31G(d) level of theory [10]. The general expression for G3X contains corrections for diffuse (ΔE_+) and polarization ($\Delta E_{2df,p}$) functions, electron correlation effects ($\Delta E_{QCISD(T)}$), effects from the size of the basis set ($\Delta E_{G3large}$), and improvement beyond the G3large basis set (ΔE_{HF}), spin–orbit correction (E_{SO}) from the literature, zero point energy (ZPE) and thermal effects (E_{ZPE}), and an empirical higher level correction (E_{HLC}).

In this method, the molecular equilibrium geometries were obtained from B3LYP/6-31G(2df,p). The ZPE is also obtained from the harmonic approximation at the B3LYP/6-31G(2df,p) level, and the frequencies are scaled by a factor of 0.9854 [15].

EnAt1 and EnAt2 arise from the junction of the G3X and G3X(CCSD) with pseudopotential, and the scaling of the experimental atomization energies was used. These experimental energies were adjusted to minimize the MAD between the calculated and experimental data. The mean absolute deviation of a dataset is the mean distance between each data point and the mean. This shows us the variability in a dataset. $MAD = (\sum_{i=1}^{n} |\Delta H_f^o (i; exp) - \Delta H_f^o (i; method)|) / n$.

All calculations were performed by using the Gaussian 09 package of programs [36].

2 Results and discussion

Table 1 contains the enthalpy of formation for compounds of sodium, lithium and magnesium, calculated using G3X-CEP, G3X(CCSD)-CEP, G4, EnAt1, EnAt2, G3B3, G3MP2B3 and CBS-QB3 and compared to experimental data. The resulting deviation is also reported in Table 1 and Fig. 1. Comparing the MADs, EnAt1 and EnAt2 result in MADs of 3.7 kcal mol^{-1}, respectively, while G3X(CCSD)-CEP, G3X-CEP, G4, G3B3, G3MP2B3 and CBS-QB3 result in MADs of 3.9, 3.8, 2.6, 2.9, 3.7 and 4.3 kcal mol^{-1}, respectively. The difference between the general performance of calculations with G4 and CBS-QB3 is 1.7 kcal mol^{-1}. The enthalpy of formation obtained by EnAt1 and EnAt2 are computationally more economical procedures than the Gaussian-4 protocol.

Of the composite methods assessed, EnAt1 and EnAt2 perform one of the best with MADs of 3.7 kcal mol^{-1}, respectively. In many cases, they perform well, but they occasionally have large errors. Of the other methods examined, CBS-QB3 performed considerably worse than EnAt1 and EnAt2, with a MAD of more than 5 kcal mol^{-1}. A total of 43% of the enthalpies of formation calculated with CBS-QB3 showed a deviation between ± 2 kcal mol^{-1}. A greater percentage (59%) was obtained for the results calculated with EnAt1 and EnAt2. Calculations using G4 also concentrated deviations above ± 2 kcal mol^{-1} in only 41% of results, while 50% and 52% of the results were observed for EnAt1 and EnAt2, respectively.

Some results from the literature are calculated at an equivalent level and can be partially compared with those obtained using the EnAt1 and EnAt2 calculations. Caldeira and Custodio [37] performed calculations of Li_2 at the B3LYP/6–31 + G(2df,p), B3LYP-MCM1 and B3LYP-MCM2, with a deviation of -4.1, -4.2 and -4.9 kcal mol^{-1}, respectively, and EnAt1 and EnAt2 with a deviation of 1.5 and 0.0 kcal mol^{-1}, respectively. The EnAt1 and EnAt2 results offered significant increases in accuracy compared with B3LYP in different basis sets.

The MAD of Gn-CEP (EnAt1, EnAt2, G3X-CEP and G3X(CCSD)-CEP) atomization-based estimates are lower than the corresponding G4, G3B3, G3MP2B3 and CBS-QB3 atomization-based estimates, deviating by 4.2–5.8 kcal mol^{-1}. Estimates of the heat of formation value for $MgCl_2$ from the G3B3 and G3MP2B3 calculations deviated by 0.0 and 5.3 kcal mol^{-1}, respectively. These values are still better than the B3LYP/6–311 + + G(2d,2p) and OpB3LYP/6–311 + + G(2d,2p) values calculated by Lu [38], with a deviation of -9.5 and -9.1 kcal mol^{-1}, respectively.

The heats of formation values at 0 K for G3X-CEP, G3X(CCSD)-CEP, G4, B2PLYP, BMK, M06, M06-HF, LC-wPBE, PBE0, wB97XD, O3LYP and mPW1PW91: H (51.63 ± 0.001), B (136.2 ± 0.2), Li (37.69 ± 0.2), Be (76.48 ± 1.2), C (169.98 ± 0.1), N (112.53 ± 0.02), O (58.99 ± 0.02), F (18.47 ± 0.007), Na (25.69 ± 0.17), Al (78.23 ± 1.00), S (65.66 ± 0.06) and Cl (28.59 ± 0.001). However, Silva and Custodio [15] proposed the possibility of refining the calculated enthalpies of formation with respect to accurate experimental data by scaling these values at 0 K to create EnAt1 and EnAt2. The adjusted values at 0 K for EnAt1 are: H (51.57), B (134.43), Li (37.56), Be (77.32), C (170.18), N (112.61), O (59.35), F (18.73), Na (26.73), Al (83.12), S (65.52) and Cl (28.41), and values at 0 K for EnAt2 are: H (51.61), B (135.08), Li (38.30), Be (77.16), C (170.01), N (112.37), O (59.17), F (18.60), Na (26.92), Al (82.76), S (66.12) and Cl (28.47).

As shown in Supporting Information Table S.1, for the basis set aug-cc-pVDZ, BMK exhibits better performance than the other functionals (Fig. 2). The MAD of BMK is

Table 1 Comparison of EnAt1, EnAt2, G3X(CCSD)-CEP, G3X-CEP, G4, G3B3, G3MP2B3 and CBS-QB3

	Experiment—theory (kcal mol^{-1})								ΔH_f (298 K)
	EnAt1	EnAt2	G3X(CCSD)-CEP	G3X-CEP	G4	G3B3	G3MP2B3	CBS-QB3	Experimental[a]
NaAlF4	−6.0	−5.6	0.2	0.1	−4.6	−5.5	−24.9	−21.2	−440 ± 3
$BNaO_2$	−2.9	−3.5	−3.2	−3.5	−5.0	−3.3	−4.6	−6.9	−155 ± 3
Na_2Br_2	−3.6	−3.9	−2.0	−2.3	2.5	4.9	1.7	5.0	−116.2 ± 0.9
NaBr	−0.3	−0.4	0.5	0.4	0.9	−1.0	2.1	3.4	−34.4 ± 0.5
NaCN	−8.9	−12.1	−8.0	−7.8	−10.8	−8.6	−8.2	−12.4	22.5 ± 0.2
NaH	−3.1	−3.0	−2.5	−2.5	−2.8	−2.8	−2.3	−4.3	30 ± 4.5
Na^-	1.7	−1.6	3.2	3.2	−0.4	2.0	5.4	0.1	11.5 ± 0.2
Na^+	4.1	3.9	4.8	4.8	1.3	1.9	4.4	1.6	145.6 ± 0.2
NaO	−1.3	−1.7	−0.7	−0.5	−0.9	−0.3	0.5	3.8	20 ± 10
NaOH	3.6	3.3	4.7	4.8	−1.7	−0.5	0.0	−3.9	−47 ± 1.91
Na_2	0.0	−0.4	4.5	2.1	1.1	3.5	3.3	−0.7	34 ± 0.3
Na_2^-	1.0	3.8	6.4	3.2	3.9	5.7	7.6	4.8	25 ± 0.35
NaF	1.7	0.7	0.8	1.7	0.2	0.4	0.1	−2.9	−69.4 ± 0.5
NaCl	−0.7	−1.0	1.3	0.1	−0.3	0.8	1.6	0.6	−43.4 ± 0.5
$MgBr_2^+$	−1.2	−1.0	1.4	0.7	2.6	−0.1	−0.2	12.5	174.7 ± 4.5
$MgCl_2$	0.0	0.0	−0.3	1.7	1.9	0.0	0.4	6.0	−93.8 ± 1.2
Mg_2Cl_4	−0.6	−0.7	0.0	−0.5	6.5	2.1	0.9	12.8	−228.1 ± 9.0
MgClF	−1.9	−2.7	−1.5	−1.5	−0.2	−2.4	−2.2	2.7	−136 ± 5.0
MgF_2^+	11.3	11.2	13.8	14.1	15.3	12.5	12.4	18.0	141.5 ± 8.9
Mg_2F_4	−3.8	−3.3	3.4	3.5	1.3	−2.4	−4.0	3.1	−410 ± 9.0
MgF^+	−8.3	−8.2	−5.2	−5.1	6.0	−8.8	−6.7	−2.4	122.4 ± 11.0
Mg_2Br_4	−10.5	−10.2	−9.7	−10.0	2.9	0.4	−2.5	18.2	−183.5 ± 5.5
$MgBr_2$	−3.9	−3.8	−3.6	−3.9	0.8	−0.6	−1.2	8.9	−72.4 ± 2.5
MgBr	−10.7	−10.6	−7.9	−8.0	−6.1	−8.2	−7.7	−2.2	−8.5 ± 10.0
MgF_2	0.2	0.4	3.8	3.8	1.8	−0.4	−0.4	3.5	−173.7 ± 0.5
MgF	−6.7	−6.6	−3.6	−3.5	−3.3	−5.9	−5.2	−3.5	−56.6 ± 2.4
Mg^+	0.2	0.3	2.9	2.9	−0.4	−3.3	−2.6	1.4	213 ± 0.3
MgOH	−12.1	−12.1	−9.0	−8.9	−8.4	−11.7	−11.3	−8.9	−39.4 ± 7.8
$MgOH^+$	−4.3	−4.2	−1.2	−1.0	−1.9	−5.1	−3.8	1.1	139.7 ± 15
$MgCH_4$	3.3	3.4	5.8	5.8	2.2	0.6	0.0	1.5	28.4 ± 7.0
$MgNH_3$	2.1	2.2	5.5	5.5	1.6	−6.3	−1.8	0.4	14.8 ± 6.0
Li_2Cl_2	8.9	7.4	9.0	8.7	−1.2	−0.4	−1.8	0.2	−143 ± 5.0
LiF	−0.3	−0.9	−0.7	0.5	0.5	0.3	−0.2	0.3	−80.1 ± 2.0
Li_2F_2	1.3	−0.3	1.8	1.9	−3.0	−1.1	−3.6	−3.5	−22 ± 5.4
Li_3F_3	1.3	−0.9	2.1	2.2	−3.7	0.7	−4.1	−3.9	−36 ± 2.6
LiHO	13.7	12.8	14.0	14.1	1.0	1.2	0.4	1.4	−56 ± 1.2
Li_2O	10.4	8.4	10.5	11.0	−4.0	−3.9	−4.6	−4.7	−40 ± 0.35
LiBr	6.7	6.0	6.8	6.6	−1.7	−1.0	−1.6	1.8	−36.8 ± 0.02
Li^-	2.1	1.4	2.9	2.9	−0.6	1.7	6.3	−0.4	22.3 ± 0.02
LiCl	−0.4	1.2	−1.0	2.1	−1.4	−1.0	−1.2	0.1	−46.8 ± 3.0
$LiCl^-$	1.4	0.2	1.2	4.2	0.3	0.9	1.9	0.4	−60.4 ± 0.5
LiBeH	−0.3	0.0	0.2	0.2	2.3	1.5	−1.3	0.5	75.8 ± 0.01
$LiCH_3$	0.3	0.3	0.1	0.1	0.6	0.6	0.1	−0.6	25.2 ± 0.01
LiH	−0.2	−0.5	0.5	−0.4	0.5	0.4	0.0	−0.3	33.3 ± 0.01
LiNa	−0.8	0.0	3.8	0.1	0.6	3.2	3.4	0.4	43.4± 1.52
Li_2	1.5	0.0	2.6	1.3	−0.3	2.4	3.1	0.2	51.6 ± 0.7
MAD	3.7	3.7	3.9	3.8	2.6	2.9	3.7	4.3	
%(−2 ≥ ΔE ≤ 2)	50	48	40	37	59	48	46	43	
%(−2 < ΔE and ΔE > 2)	50	52	60	63	41	52	54	57	

Methods for Calculation of ΔH_f (298 K) for a Test Set of 46 Molecules

[a]Data from ref [39] (298.15 K)

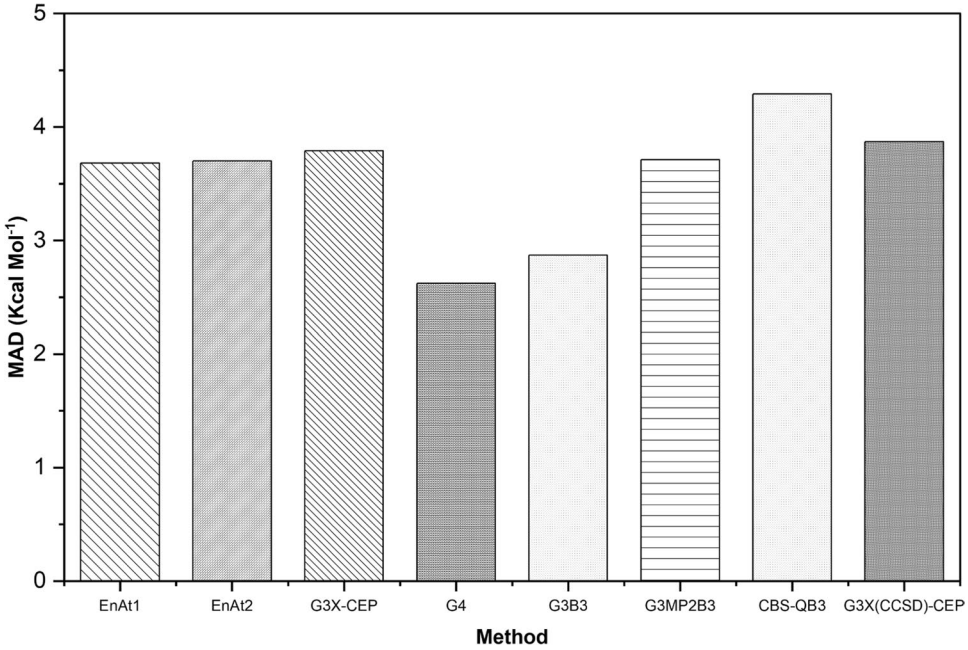

Fig. 1 MAD of Selected composite methods

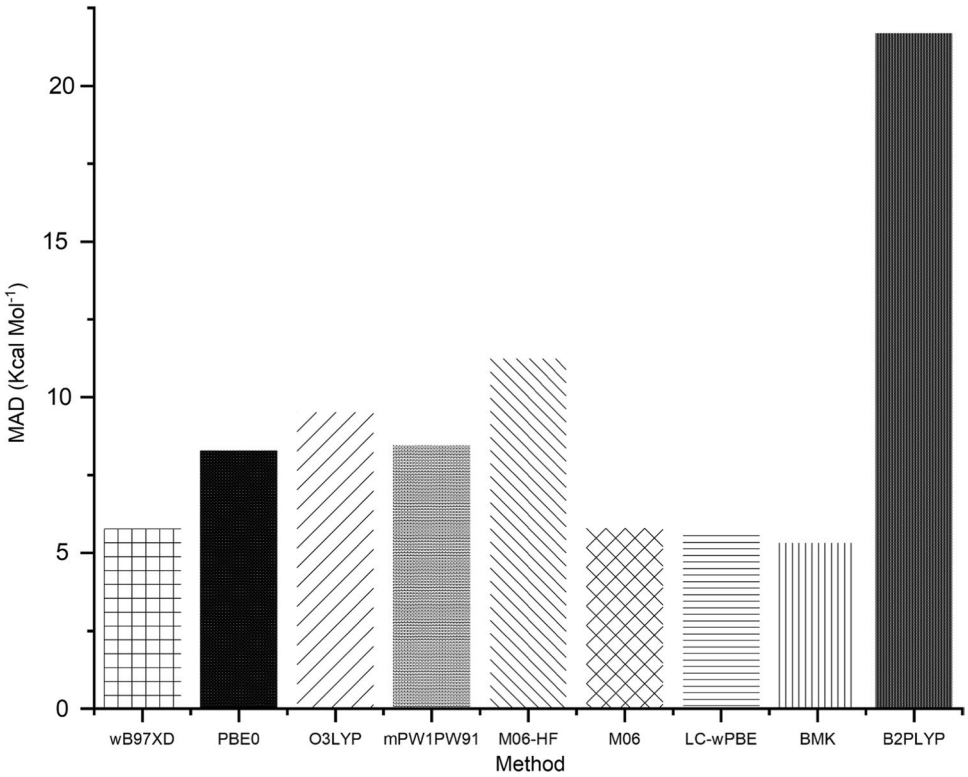

Fig. 2 MAD of Selected Density Functional Methods with aug-cc-pVDZ

5.3 kcal mol^{-1}, which is significantly lower than that of B2PLYP at 21.7 kcal mol^{-1}. M06, M06-HF, LC-wPBE, PBE0, wB97XD, O3LYP and mPW1PW91 atomization-based estimates deviate by 5.6–14.8 kcal mol^{-1}. It should be pointed out that Li_2F_2 and Li_3F_3 provide significant contributions to the MAD of the functionals: for BMK, the calculated deviations of these three compounds are -6.4 and -9.5 kcal mol^{-1}, respectively. This performance was ascribed to the poor LiF-LiF interaction in the functionals.

As shown in Supporting Information Table S.2, we studied the behaviour of M06-HF for a test set. This method shows basis set dependence more than wB97XD and M06. LC-wPBE is for the aug-cc-pVTZ basis set; the MAD reaches its smallest value at 10.5 kcal mol^{-1} (Fig. 3). When

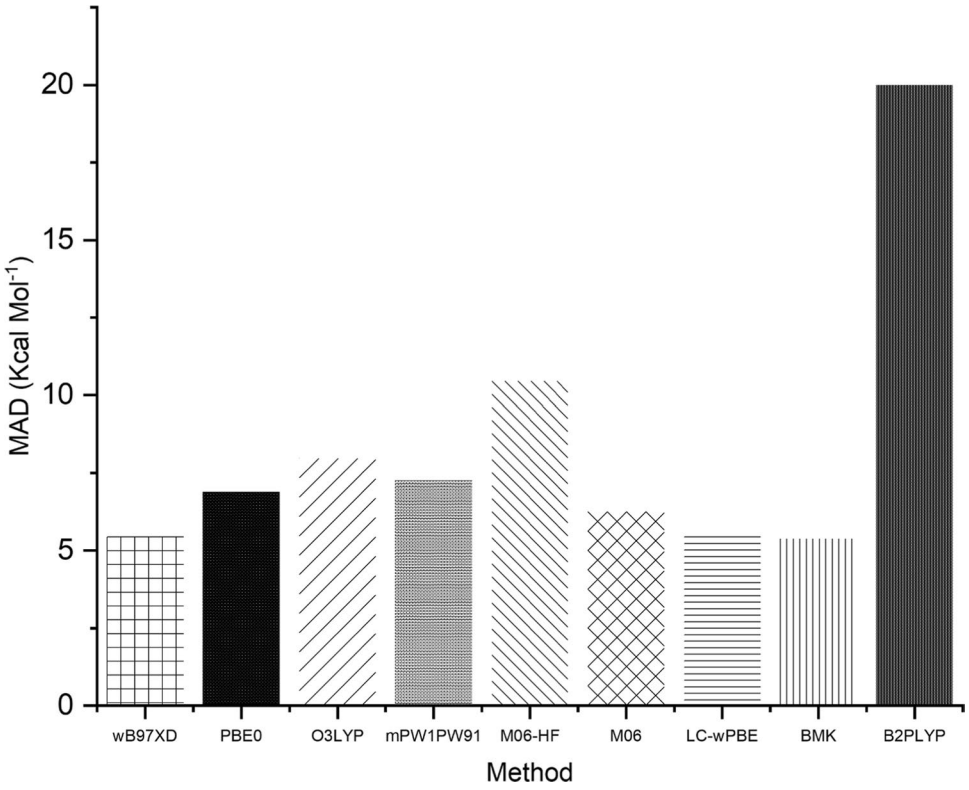

Fig. 3 MAD of Selected Density Functional Methods with aug-cc-pVTZ

the basis set is decreased to the aug-cc-pVDZ level, the MAD becomes 11.2 kcal mol^{-1}. The deviations distribution of enthalpies of formation used to evaluate the performance of M06-HF in detail are shown in Table S.2. Nearly 9% of deviations fall within ± 2 kcal mol^{-1} of experimental values, and 91% of deviations are above ± 2 kcal mol^{-1} of experimental values. However, the other functionals had less than 28% of deviations fall within ± 2 kcal mol.$^{-1}$

The accuracy of extrapolation(1) can be compared among the calculations using the respective functionals and the aug-cc-pVDZ and aug-cc-pVTZ basis sets. The best results were obtained using LC-wPBE/extrapolation(1), which yielded accuracy superior to the other functionals with extrapolation(1). However, measuring the value of the energies set test with respect to the functionals and the aug-cc-pVDZ for aug-cc-pVTZ basis sets, the errors were not systematically reduced with the enlargement of the basis set. For example, M06/aug-cc-pVTZ results in a MAD of 5.9 kcal mol^{-1} and extrapolation(1) results in a MAD of 5.9 kcal mol^{-1}. Nevertheless, performance of the extrapolation(1) is compatible with the results obtained with the respective functionals and aug-cc-pVDZ and aug-cc-pVTZ basis sets. The deviations distribution of enthalpies of formation of functionals with extrapolation(1) are given in Table 2. Nearly 7%-28% of deviations fall within ± 2 kcal mol^{-1} of experimental values, but between 37%-59% fall within ± 2 kcal mol^{-1} of experimental values for composite methods.

We have also examined the extrapolation(3) proposals of Chinini and Custodio for the 46-molecule set in Table 3. The results are compatible with the results obtained with extrapolation(1). EnAt1 and EnAt2 exhibit much better performance than the functionals with extrapolation(1) and extrapolation(3). The 46 enthalpies calculated (Table 3) show a tendency towards larger dispersion of the results for extrapolation(3) when compared to the EnAt1 and EnAt2 methods. For example, the distribution for M06-HF indicates that 4% of the presented cases correspond to 2 molecule accuracy in the range of ± 2 kcal mol^{-1}, and 26% of the test set calculated with BMK showed a deviation between ± 2 kcal mol^{-1}.

Similarly, in results reported by Grimme [20], the TPShS/TZV2P and B2PLYP/TZV2P methods calculated deviations of 1.0 and -1.0 kcal mol^{-1} for LiH, respectively. In the present work, we found results corresponding to Grimme for wB97XD (0.7 kcal mol^{-1}), O3LYP (1.9 kcal mol^{-1}), M06 (1.8 kcal mol^{-1}), LC-wPBE (-1.3 kcal mol^{-1}) and BMK (0.2 kcal mol^{-1}) for extrapolation(3). Some papers showed M06-HF and M06 (the two hybrid meta-GGA exchange–correlation functionals) are the best functionals for thermochemistry calculations when compared to other functionals, but this fact was not demonstrated in this work. LC-wPBE and BMK showed the best MAD for aug-cc-pVDZ, aug-cc-pVTZ, extrapolation(1) and extrapolation(3).

As shown in Supporting Information Table S.3, for the basis set aug-cc-pVQZ, BMK exhibits better performance than the other functionals (Fig. 4). The MAD of BMK is

Table 2 Comparison of selected density functional methods (Extrapolation(1)) on the 46-molecule test set

	experiment—theory (kcal mol^{-1})									ΔH_f (298 K)
	wB97XD	PBE0	O3LYP	mPW1PW91	M06-HF	M06	LC-wPBE	BMK	B2PLYP	Experimental[a]
NaAlF4	−14.4	−22.7	−33.3	−30.2	1.0	−3.0	−7.6	−6.2	−71.3	−440 ± 3
$BNaO_2$	0.7	0.5	−10.2	−7.7	−13.0	10.9	2.7	12.5	−51.3	−155 ± 3
Na_2Br_2	3.0	6.1	−13.5	−5.6	6.6	0.4	−3.3	−4.6	−20.2	−116.2 ± 0.9
NaBr	2.5	4.1	−3.6	−1.3	2.6	1.7	−0.5	0.2	−8.7	−34.4 ± 0.5
NaCN	−3.7	−2.8	−12.6	−10.7	−6.8	−2.0	−1.7	−9.2	−45.2	22.5 ± 0.2
NaH	−1.5	−1.5	−1.0	−6.6	−8.3	0.5	−5.4	−5.8	−10.2	30 ± 4.5
Na^-	−2.5	2.7	−1.6	−3.2	−2.8	−3.2	−3.5	−7.1	−7.6	11.5 ± 0.2
Na^+	5.3	−1.0	−2.7	−2.2	−10.9	8.3	−0.7	−0.8	0.0	145.6 ± 0.2
NaO	−0.4	−0.1	−4.3	−5.5	−10.4	3.4	−0.1	0.0	−17.6	20 ± 10
NaOH	2.6	−0.1	−2.3	−6.0	−3.8	5.6	0.9	3.1	−27.7	−47 ± 1.91
Na_2	−0.8	−0.2	1.5	−12.4	−3.9	1.6	−4.1	−6.2	−6.3	34 ± 0.3
Na_2^-	−0.9	−13.1	1.6	−24.9	−0.3	−0.1	0.0	−7.1	−7.5	25 ± 0.35
NaF	−0.6	−2.1	−4.8	−7.3	−8.0	4.5	−0.1	0.2	−20.2	−69.4 ± 0.5
NaCl	0.9	0.5	−5.6	−4.9	−5.9	4.3	−3.2	1.3	−13.1	−43.4 ± 0.5
$MgBr_2^+$	11.8	14.3	9.3	12.6	5.3	15.0	4.9	7.7	0.1	174.7 ± 4.5
$MgCl_2$	3.5	1.4	−3.9	0.0	6.7	4.7	3.2	3.2	−14.3	−93.8 ± 1.2
Mg_2Cl_4	5.5	1.8	−16.2	−2.1	19.4	8.8	5.9	6.6	−32.0	−228.1 ± 9.0
MgClF	−0.9	−4.9	−6.9	−6.0	2.7	1.9	2.2	−1.8	−23.9	−136 ± 5.0
MgF_2^+	27.0	21.1	24.4	19.8	2.9	31.5	24.6	20.9	−2.4	141.5 ± 8.9
Mg_2F_4	−6.4	−17.0	−21.3	−19.4	11.4	2.7	7.0	−5.4	−60.2	−410 ± 9.0
MgF^+	−2.2	−9.9	−8.6	−10.3	−10.8	1.6	−3.1	−6.7	−18.9	122.4 ± 11.0
Mg_2Br_4	4.9	7.7	−16.9	4.0	42.2	−6.2	8.5	−3.9	−24.6	−183.5 ± 5.5
$MgBr_2$	4.1	5.6	−2.9	4.1	19.0	−2.2	5.4	−22.8	−9.1	−72.4 ± 2.5
MgBr	−4.3	−1.4	−7.2	−2.0	9.1	−10.3	−1.0	−6.1	−8.4	−8.5 ± 10.0
MgF_2	−0.8	−6.8	−5.7	−7.5	2.8	3.8	5.6	−1.5	−29.1	−173.7 ± 0.5
MgF	−4.5	−5.4	−6.6	−5.7	3.1	−5.5	1.6	−4.2	−15.9	−56.6 ± 2.4
Mg^+	4.4	3.5	1.6	3.2	7.2	2.5	4.4	4.1	8.9	213 ± 0.3
MgOH	−4.6	−6.1	−6.7	−7.1	5.2	−7.2	0.0	−4.0	−26.5	−39.4 ± 7.8
$MgOH^+$	6.8	−0.3	2.3	−1.5	2.3	8.8	5.1	2.9	−19.1	139.7 ± 15
$MgCH_4$	27.5	25.3	28.6	23.5	30.2	26.9	25.7	19.3	−4.5	28.4 ± 7.0
$MgNH_3$	19.7	14.5	17.2	14.0	21.6	15.9	25.6	11.2	−14.0	14.8 ± 6.0
Li_2Cl_2	−6.6	−9.4	−15.3	−10.6	−10.4	−1.9	−9.8	−0.5	−25.9	−143 ± 5.0
LiF	−2.4	−22.4	−2.2	−4.8	−4.2	3.0	0.3	2.7	−16.4	−80.1 ± 2.0
Li_2F_2	−9.9	−20.2	−15.0	−15.7	−10.1	−2.1	−5.8	−0.6	−36.9	−22 ± 5.4
Li_3F_3	−14.9	−19.5	−19.9	−22.2	−15.1	−2.1	−7.8	−0.7	−52.9	−36 ± 2.6
LiHO	4.6	1.0	4.4	0.2	3.5	7.2	4.7	9.0	−20.3	−56 ± 1.2
Li_2O	−8.2	−10.5	−9.5	−11.4	−10.5	−1.2	−6.2	−1.0	−32.8	−40 ± 0.35
LiBr	−1.5	57.8	−3.7	5.6	5.5	−2.8	−2.3	−0.1	−8.2	−36.8 ± 0.02
Li^-	−3.8	−4.4	−3.6	−4.3	−4.2	−3.3	−4.6	−7.2	−9.2	22.3 ± 0.02
LiCl	−2.1	−3.5	−4.4	−3.8	−3.7	0.7	−3.8	2.0	−11.3	−46.8 ± 3.0
$LiCl^-$	−2.2	−1.8	−3.9	−2.0	−150.1	−6.8	−1.9	−1.1	−12.2	−60.4 ± 0.5
LiBeH	7.9	3.7	7.3	4.3	−4.5	11.9	−5.4	3.7	−0.4	75.8 ± 0.01
$LiCH_3$	19.5	18.3	21.6	17.0	18.0	21.5	15.3	16.0	−9.7	25.2 ± 0.01
LiH	0.6	−3.0	1.7	−2.5	−4.5	1.8	−1.6	0.1	−4.8	33.3 ± 0.01
LiNa	−1.6	2.4	−0.1	−3.9	−4.7	1.6	−4.5	−6.6	−7.0	43.4 ± 1.52
Li_2	−3.7	−5.8	−3.5	−5.0	−6.5	0.6	−5.5	−7.4	−8.0	51.6 ± 0.7
MAD	5.8	8.1	8.7	9.5	11.7	5.9	5.4	5.5	19.0	
$\%(-2 \geq \Delta E \leq 2)$	26	28	15	11	4	28	28	33	7	

Table 2 (continued)

	experiment—theory (kcal mol^{-1})									ΔH_f (298 K)
	wB97XD	PBE0	O3LYP	mPW1PW91	M06-HF	M06	LC-wPBE	BMK	B2PLYP	Experimental[a]
%(−2 < ΔE and ΔE > 2)	74	72	84	89	96	72	72	67	93	

[a]Data from ref [39] (298.15 K)

5.4 kcal mol^{-1}, which is significantly lower than that of B2PLYP at 20.0 kcal mol^{-1}. M06, M06-HF, LC-wPBE, PBE0, wB97XD, O3LYP and mPW1PW91 atomization-based estimates deviate by 5.4–10.5 kcal mol^{-1}.

The accuracy of extrapolation(2) can be compared among the calculations using the respective functionals and the aug-cc-pVTZ and aug-cc-pVQZ basis sets. The best results were obtained using wB97XD/extrapolation(2) and BMK/extrapolation(2), which yielded accuracy superior to the other functionals with extrapolation(2). The results are compatible with the results obtained with extrapolation(2) with aug-cc-pVTZ and aug-cc-pVQZ basis sets. The extrapolation(4) (with aug-cc-pVTZ and aug-cc-pVQZ) proposals of Chinini and Custodio for the 46-molecule set in Table S.5. The results are compatible with the results obtained with extrapolation(3) with aug-cc-pVDZ and aug-cc-pVTZ.

Two thermochemical conventions are known for the electron in ionisation and electron attachment. One is called the electron thermal convention, which treats the electron as a chemical element, and the other is called the ion convention, which shows the electron as a subatomic particle. The "ion convention" is used in the present work [39].

In many papers, the non-hydrogenated compounds were responsible for the largest deviations for functionals and composite methods. The 36 non-hydrogenated compounds presented the worst results. These values denote system irregularities, where functionals, methods and basis sets are inadequate to report subtle structural and electronic effects. Non-hydrogenated compounds and molecules containing transition metals are usually a source of large deviations. These anomalous deviations have been easily reported and, so far, have not been solved by functionals and basis sets. It is known that the heat of formation for compounds containing these atoms show a variety of large positive and negative deviations with respect to experimental data. In recent years, composite methods have become a great alternative for the calculation of thermochemical properties, with a low computational cost and applicability to chemical systems. These methods have some additive corrections to the order of electronic correlations, and some have extrapolation techniques.

It is important to keep in mind that part of the excellent agreement with experimental for the composite methods tested in this paper arise from a cancellation of errors, as for example, those appearing from zero-point energy, geometry, truncation in the one- and n-particle basis sets, and neglect of core-core and core-valence correlation. Furthermore, the experimental values are generally accurate to just about 1 kcal mol^{-1}. To explain why some composite methods or some basis sets than others will require accurate benchmarking, where the error associated with every approximation is tested in detail.

The composite methods have spin–orbit correction and DFT ones do not. For the chlorine and fluorine containing molecules, all of the atomization energies are extra-large. Insertion of the spin–orbit correction reduces the atomization energies of the chlorine and fluorine substituted molecules. In composite methods, it is known that incorporation of the spin–orbit correction results in better agreement between theory and experimental for the first-row fluorides, but not the second-row fluorides. We are aware there is little motive to question the security of the experimental data for the fluorine molecules.

One of the advantages of composite methods is to improve the correlation energy treatment. Gaussian-3 calculations were carried out. The G3//B3 model produces effective QCISD(T) total energies calculated with the G3large basis set, which includes core polarization functions (for example, 3d2f polarization functions for chlorine atoms). The G3 e G4 based treatments are always expected to give more accurate results when compared to functionals.

We must keep in mind that the accuracy of composite methods and functionals has improved to the point where it is now necessary to be more prudent in our assessment criteria of these methods. One of the major problems of formation heat calculations is doubt and mistrust in the heat of experimental formation. We insert the uncertainty in the experimental heats of formation of molecules. Also, the uncertainty in the calculated heats of formation show up from the uncertainty in the experimental heats of formation of the constituent atoms.

Given their relevance, it is known to everyone that heats of formation for several atoms, for example, B, Be, and Si, are notoriously imprecise [40]. Boron is the most curious case, where the accepted JANAF experimental enthalpy formation $B_{(g)}$ values are 135 ± 1 kcal mol^{-1} and 133.8 kcal mol^{-1}. This error is due to complications involving metallic impurities. A much higher value of 136.2 (± 0.2 kcal mol^{-1}) was rejected by the JANAF compilers and indicated by the Gaussian.

Table 3 Comparison of selected density functional methods (extrapolation(3)) on the 46-molecule test set

	experiment—theory (kcal mol $^{-1}$)									ΔH_f (298 K)
	wB97XD	PBE0	O3LYP	mPW1PW91	M06-HF	M06	LC-wPBE	BMK	B2PLYP	Experimental[a]
NaAlF4	−12.9	−26.4	−31.6	−28.5	3.9	−1.7	−5.7	−5.8	−69.6	−440 ± 3
$BNaO_2$	1.4	−4.1	−9.3	−6.9	−12.8	11.5	3.6	12.7	−50.3	−155 ± 3
Na_2Br_2	2.6	−5.2	−13.7	−5.9	5.7	−0.2	−3.6	−4.7	−20.5	−116.2 ± 0.9
NaBr	2.4	−1.5	−3.7	−1.4	2.2	1.4	−0.6	0.2	−8.7	−34.4 ± 0.5
NaCN	−2.2	−7.3	−11.9	−9.5	−6.3	−1.1	−1.8	−9.8	−44.2	22.5 ± 0.2
NaH	−1.4	−6.9	−1.0	−6.5	−8.1	0.5	−5.3	−5.8	−10.1	30 ± 4.5
Na^-	−2.5	−2.8	−1.6	−3.2	−2.8	−3.2	−3.5	−7.1	−7.6	11.5 ± 0.2
Na^+	5.4	−7.0	−2.7	−2.2	−11.1	8.2	−0.8	−0.8	0.0	145.6 ± 0.2
NaO	−0.4	−5.6	−4.3	−5.5	−10.2	3.2	−0.1	0.1	−17.6	20 ± 10
NaOH	2.7	−5.4	−2.1	−5.8	−3.2	5.5	1.1	3.2	−27.5	−47 ± 1.91
Na_2	−0.8	−11.2	1.5	−12.4	−4.2	1.6	−4.1	−6.2	−6.3	34 ± 0.3
Na_2^-	−0.9	−24.1	1.5	−24.9	−0.5	−0.1	0.0	−7.1	−7.5	25 ± 0.35
NaF	−0.6	−7.6	−4.8	−7.3	−7.7	4.4	−0.1	0.3	−20.2	−69.4 ± 0.5
NaCl	0.8	−5.0	−5.6	−5.0	−5.3	4.0	−3.2	1.3	−13.2	−43.4 ± 0.5
$MgBr_2^+$	12.1	13.8	9.6	12.9	5.7	15.5	5.5	7.8	−0.4	174.7 ± 4.5
$MgCl_2$	3.9	1.0	−3.4	0.4	9.1	4.9	4.0	3.2	−14.7	−93.8 ± 1.2
Mg_2Cl_4	6.2	0.9	−15.2	−1.4	24.3	8.9	7.3	6.2	−32.8	−228.1 ± 9.0
MgClF	−0.7	−5.4	−6.6	−5.7	4.9	2.0	2.8	−1.7	−24.4	−136 ± 5.0
MgF_2^+	27.1	20.5	24.2	19.9	3.4	31.7	25.2	21.0	−3.1	141.5 ± 8.9
Mg_2F_4	−6.3	−18.2	−20.9	−19.0	15.1	2.6	8.2	−5.2	−61.5	−410 ± 9.0
MgF^+	−2.0	−10.5	−8.5	−10.0	−9.4	1.8	−2.6	−6.6	−19.5	122.4 ± 11.0
Mg_2Br_4	5.1	6.5	−16.4	4.3	43.0	−6.0	9.4	−3.8	−25.8	−183.5 ± 5.5
$MgBr_2$	4.3	5.5	−2.6	4.3	19.5	−2.0	6.0	−0.3	−9.6	−72.4 ± 2.5
MgBr	−4.3	−2.1	−7.1	−1.9	9.9	−10.3	−0.6	−6.0	−9.1	−8.5 ± 10.0
MgF_2	−0.7	−7.4	−5.6	−7.3	4.6	3.8	6.2	−1.4	−29.7	−173.7 ± 0.5
MgF	−4.5	−6.1	−6.5	−5.7	4.6	−5.4	2.1	−4.1	−16.6	−56.6 ± 2.4
Mg^+	4.5	2.8	1.6	3.3	8.5	2.6	4.8	4.1	8.1	213 ± 0.3
MgOH	−4.3	−6.5	−6.4	−6.8	7.1	−7.1	0.7	−4.0	−27.0	−39.4 ± 7.8
$MgOH^+$	7.2	−0.7	2.7	−1.0	4.1	9.0	5.9	2.9	−19.4	139.7 ± 15
$MgCH_4$	28.5	25.4	29.5	24.5	33.2	27.7	25.4	19.1	−4.3	28.4 ± 7.0
$MgNH_3$	21.3	14.5	18.0	13.7	23.8	16.5	27.6	10.9	−14.0	14.8 ± 6.0
Li_2Cl_2	−6.4	−9.0	−15.1	−10.2	−8.5	−2.2	−9.2	−0.5	−25.6	−143 ± 5.0
LiF	−2.3	−4.4	−2.0	−4.5	−3.8	3.1	0.5	2.8	−16.2	−80.1 ± 2.0
Li_2F_2	−9.8	−14.3	−15.2	−15.4	−8.7	−2.4	−5.5	−0.6	−36.7	−22 ± 5.4
Li_3F_3	−14.9	−19.9	−19.9	−21.9	−13.0	−2.5	−7.2	−0.5	−52.7	−36 ± 2.6
LiHO	4.4	1.5	4.9	0.7	4.4	7.3	5.3	9.1	−19.9	−56 ± 1.2
Li_2O	−7.7	−9.9	−9.0	−10.8	−9.7	−0.6	−5.5	−0.8	−32.3	−40 ± 0.35
LiBr	−1.4	58.0	−3.5	57.8	5.4	−2.8	−2.1	−0.1	−8.1	−36.8 ± 0.02
Li^-	−3.8	−4.4	−3.6	−4.3	−4.0	−3.2	−4.6	−7.2	−9.2	22.3 ± 0.02
LiCl	−2.0	−3.3	−4.1	−3.6	−2.8	0.7	−3.6	2.2	−11.1	−46.8 ± 3.0
$LiCl^-$	−2.2	−1.8	−3.8	−2.0	−167.4	−7.5	−1.8	−1.1	−12.2	−60.4 ± 0.5
LiBeH	8.8	3.9	7.4	4.4	−4.1	12.9	−6.5	3.5	−0.3	75.8 ± 0.01
$LiCH_3$	20.3	19.3	22.4	17.8	19.8	22.1	14.6	15.8	−8.6	25.2 ± 0.01
LiH	0.7	−2.8	1.9	−2.3	−4.1	1.8	−1.4	0.2	−4.6	33.3 ± 0.01
LiNa	−1.5	−3.1	−0.2	−3.9	−4.8	1.6	−4.5	−6.6	−7.0	43.4 ± 1.52
Li_2	−3.7	−5.8	−3.5	−5.0	−6.5	0.7	−5.5	−7.4	−8.0	51.6 ± 0.7
MAD	5.8	9.3	8.6	9.4	12.6	6.0	5.6	5.0	19.0	
$\%(-2 \geq \Delta E \leq 2)$	28	13	15	15	2	30	26	33	7	

Table 3 (continued)

	experiment—theory (kcal mol $^{-1}$)									ΔH_f (298 K)
	wB97XD	PBE0	O3LYP	mPW1PW91	M06-HF	M06	LC-wPBE	BMK	B2PLYP	Experimental[a]
%(−2 < ΔE and ΔE > 2)	72	87	85	85	98	70	74	67	93	

[a]Data from ref [39] (298.15 K)

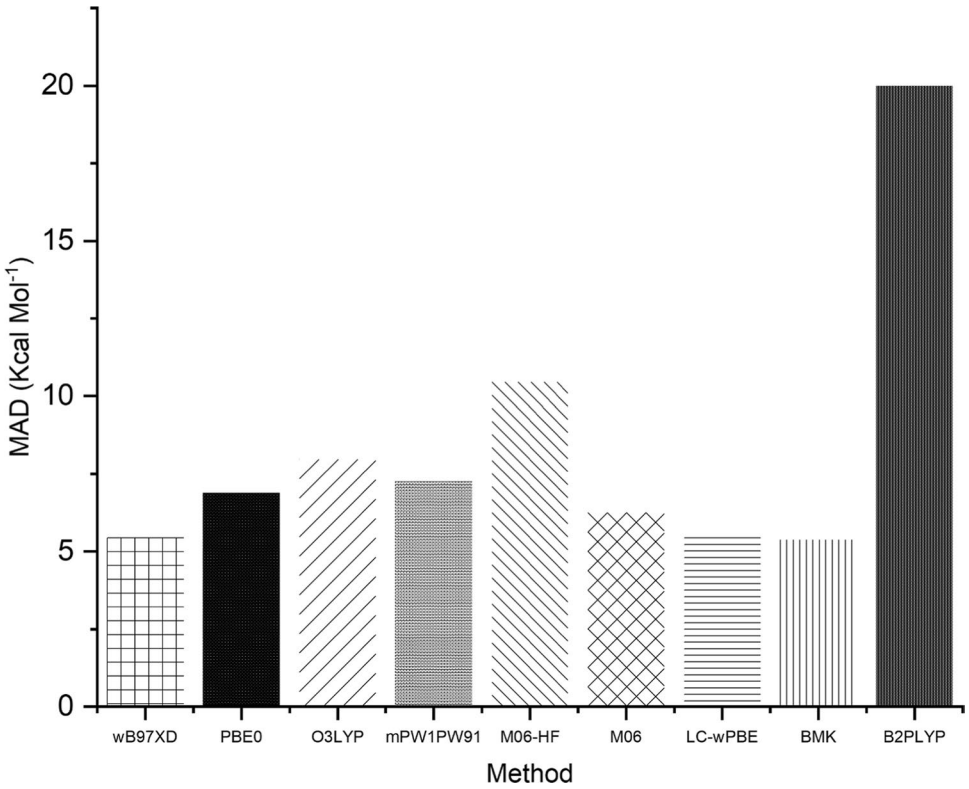

Fig. 4 MAD of Selected Density Functional Methods with aug-cc-pVQZ

This study uses scaled atomization energies to benchmark the calculated enthalpy formation with different functionals, Gaussian-n (Gn), and CBS-QB3 methods for these metallic compounds. The calculation of these different metallic compounds involving atomization processes will result in large errors just because there are a lot of correlation energies in these metallic bonds that are broken to form the atoms. It is widely documented the poor performance of different functionals in this regard.

The results clearly demonstrate that the functionals are not recommended for use in atomization for the atoms Na, Mg, and Li. Probably a better strategy to improve the results for the functional ones is the application of isodesmic enthalpy [41, 42]. The big problem in the use of isodesmic enthalpy calculations is that the value established for enthalpy formation will be subordinate in the choice of the isodesmic reaction. The strategy used by most authors is to include what are known as bond separation reactions [43] as an only determined implementation of the isodesmic reaction approach. We can say that, in this method, we separate all formal bonds between non-hydrogen atoms into the simplest parent molecules containing these same kinds of bonds. Therefore, every other bond to the wish atom pair is substituted by bonds to hydrogens, and the chemical equation is balanced by including the required single atom hydrides.

Although the G4 MAD of 2.6 kcal mol^{-1} is much larger than for the main-group molecules in the G3/05 test set (0.8 kcal mol^{-1}), the uncertainties in the experimental values are much larger for the 46 molecule set. The average uncertainty for the 46 molecule set is 2.0 kcal/mol, so the G4 MAD is near the experimental uncertainty.

The obtained EnAt1 (3.7), EnAt2 (3.7), G3X(CCSD)-CEP (3.9), G3X-CEP (3.8), G3B3 (2.9), G3MP2B3 (3.7) and CBS-QB3 (4.3) ΔH_f value is outside the experimental error bars. However, MgF_2^+ (141.5 ± 8.9) is regarded as a statistical outlier due to its large experimental uncertainty. Like the analogous, Mg_2F_4 (-410 ± 9.0) and MgF^+ (122.4 ± 11.0) may have complicated electronic structure that has not been well studied.

Figures 5 and 6 show the best DFT with bases aug-cc-pVDZ and aug-cc-pVQZ, and compared with composite methods, both have more characteristics and greater deviations for some Mg and Li molecules, and we observe that in the composite methods a greater concentration of the deviation between more ± 5 kcal mol^{-1}.

The advantage of the EnAt1 and EnAt2 calculations over G4 is the much lower CPU time. The Hartree–Fock extrapolation (aug-cc-pVQZ and aug-cc-pV5Z) technique used with G4 accounts for up to 70% of computational time and something seen with many functionals with set basis aug-cc-pVQZ and aug-cc-pV5Z [12, 14, 15]. This fact is demonstrated in the paper G4CEP and G3X-CEP. The EnAt1 and EnAt2 composite methods were developed by combining a compact effective pseudopotential (CEP) with the G3X and G3X(CCSD) all-electron methods.

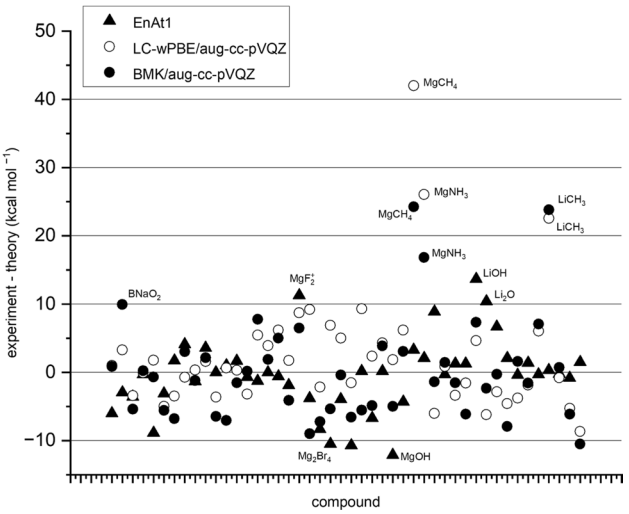

Fig. 6 Deviations of Na, Mg and Li compounds with aug-cc-pVQZ and composite method

3 Conclusion

In summary, it can be concluded that the accuracy of EnAt1 and EnAt2 for enthalpy formation is satisfactory when compared to other composite methods. In any case, EnAt1 and EnAt2 represent a successful step along a direction that can still be explored; from a more practical point of view, they are very robust and efficient in general. Heat formation was calculated for a set of widely used compounds of sodium and magnesium using a number of methods; EnAt1 and EnAt2 performed best against experimental values and are recommended for calculations.

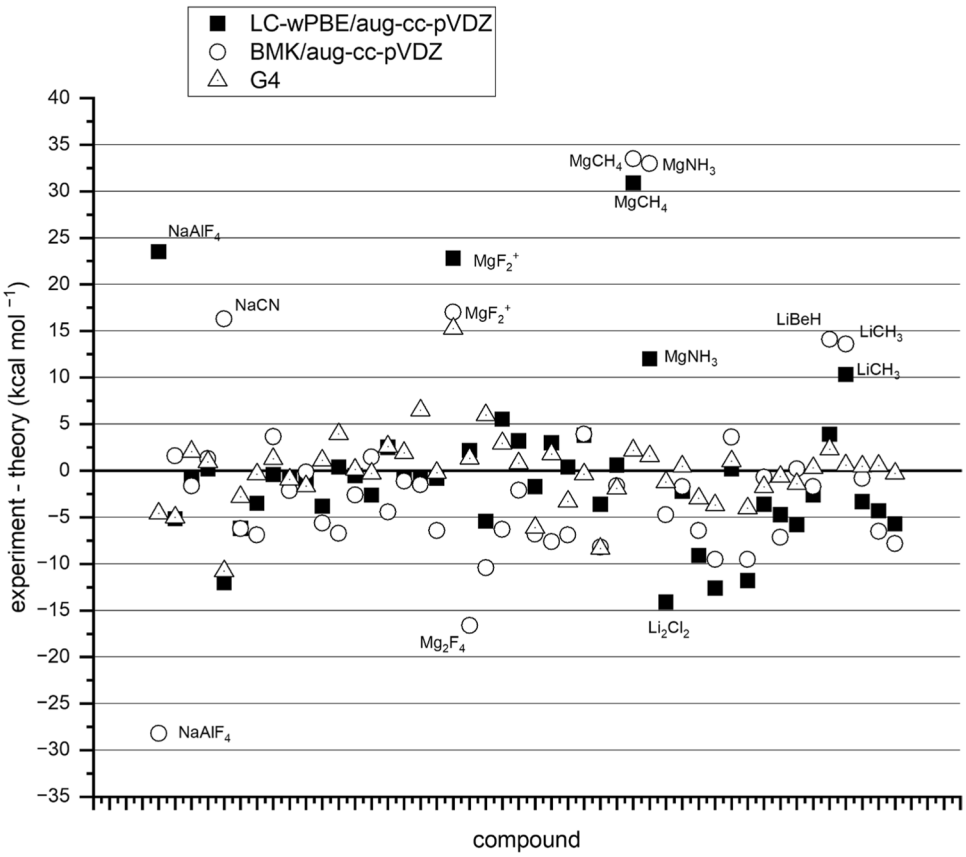

Fig. 5 Deviations of Na, Mg and Li compounds with aug-cc-pVDZ and composite method

The performance of the composite methods was benchmarked using our EnAt1 and EnAt2 heats of formation, obtaining the following MADs: EnAt1 (3.7), EnAt2 (3.7), G3X(CCSD)-CEP (3.9), G3X-CEP (3.8), G4 (2.6), G3B3 (2.9), G3MP2B3 (3.7) and CBS-QB3 (4.3). In particular, EnAt1 and EnAt2 appear to offer an excellent performance-to-computational cost ratio. In general, the agreement between enthalpy formations calculated using the G4, G3B3, G3MP2B3 and CBS-QB3 methods is extremely good when compared to functional calculations.

Extrapolation formula based exponential formulas were tested and used with many functionals for the calculation of test set enthalpies of formation. A comparative analysis of the extrapolation methods in work suggests that the use of the extrapolation approach is a reliable alternative to the optimization of heat formation, but the use of EnAt1 and EnAt2 is a more economical computational procedure.

The overall error for G4 of 2.6 kcal mol^{-1} is significantly larger than its previously reported performance for molecules containing main-group elements in the G3/05 test set. However, considering the relatively large uncertainties in the experimental enthalpies, the G4 method performs reasonably well.

Supplementary Information The online version contains supplementary material available at https://doi.org/10.1007/s00214-023-03081-x.

Acknowledgements The author would like to acknowledge The National Center of High Performance Computing in Ceará (CENAPAD-UFC) for access to their computational facilities.

Authors' contributions Not applicable.

Funding Not applicable.

Availability of data and material Not applicable.

Code Availability Not applicable.

Declarations

Conflict of interest Not applicable.

References

1. Karimov A, Orujova A, Taslimi P, et al. (2020) Novel functionally substituted esters based on sodium diethyldithiocarbamate derivatives: synthesis, characterization, biological activity and molecular docking studies. Bioorganic Chem 99. https://doi.org/10.1016/j.bioorg.2020.103762
2. Chen Z, Yang X, Fu Y (2020) Influence of sodium propargyl sulfonate on electrodeposition of Fe–Co alloy. J Alloy Compd 826:154167. https://doi.org/10.1016/j.jallcom.2020.154167
3. Shimkevich AL (2021) A true solubility versus the observed one for metal sodium in its molten chloride. Chem Phys 540:110975. https://doi.org/10.1016/j.chemphys.2020.110975
4. Dong H, Wang Y, Tang P et al (2021) A novel strategy for improving performance of lithium oxygen batteries. J Colloid Interface Sci 584:246–252. https://doi.org/10.1016/j.jcis.2020.09.096
5. Li C, He Y, Huang H (2020) Effect of lithium content on the mechanical and corrosion behaviors of HCP binary Mg–Li alloys. J Magnes Alloys. https://doi.org/10.1016/j.jma.2020.02.022
6. Hu S, Sun Y, Pu M et al (2019) Determination of boundary conditions for highly efficient separation of magnesium and lithium from salt lake brine by reaction-coupled separation technology. Sep Purif Technol 229:115813. https://doi.org/10.1016/j.seppur.2019.115813
7. Zhang F, Liu Z, Yang M et al (2020) Microscopic mechanism exploration and constitutive equation construction for compression characteristics of AZ31-TD magnesium alloy at high strain rate. Mater Sci Eng A 771:138571. https://doi.org/10.1016/j.msea.2019.1385
8. Vasiliu M, Li S, Peterson KA, Feller D, Gole JL, Dixon DA (2010) Structures and heats of formation of simple alkali metal compounds: hydrides, chlorides, fluorides, hydroxides, and oxides for Li, Na, and K. J Chem Phys 114. https://doi.org/10.1021/jp911735c
9. Vasiliu M, Feller D, Gole JL, Dixon DA (2010) Structures and heats of formation of simple alkaline earth metal compounds: fluorides, chlorides, oxides, and hydroxides for Be, Mg, and Ca. J Chem Phys 114. https://doi.org/10.1021/jp1050657
10. Curtiss LA, Redfern PC, Raghavachari K (2005) Assessment of Gaussian-3 and density-functional theories on the G3/05 test set of experimental energies. J Chem Phys 123. https://doi.org/10.1063/1.2039080
11. Curtiss LA, Redfern PC, Raghavachari K (2007) Gaussian-4 theory. J Chem Phys 126. https://doi.org/10.1063/1.2436888
12. Pereira DH, Ramos AF, Morgon NH, Custodio R (2011) Implementation of pseudopotential in the G3 theory for molecules containing first-, second-, and non-transition third-row atoms. J Chem Phys 135. https://doi.org/10.1063/1.3609241
13. Stevens WJ, Basch H, Krauss M (1984) Compact effective potentials and efficient shared-exponent basis sets for the first- and second-row atoms. J Chem Phys 81:6026–6033. https://doi.org/10.1063/1.447604
14. Silva CDS, Pereira DH, Custodio R (2016) G4CEP: A G4 theory modification by including pseudopotential for molecules containing first-, second- and third-row representative elements. J Chem Phys 144. https://doi.org/10.1063/1.4952427
15. Silva CS, Custodio R (2018) Empirical corrections in the G3X and G3X(CCSD) theories combined with a compact effective pseudopotential. Theor Chem Acc 137. https://doi.org/10.1007/s00214-018-2206-3
16. Silva CS, Custodio R (2015) Investigation of the pseudopotential Stuttgart/Dresden in the G3(MP2,CSSD,rel) theory for compounds containing transition elements. Rev Process Quím 9:66–67. https://doi.org/10.19142/rpq.v9i18.258
17. De Souza SC, Custodio R (2019) Assessment of pKa determination for monocarboxylic acids with an accurate theoretical composite method: G4CEP. J Phys Chem A 123:8314–8320. https://doi.org/10.1021/acs.jpca.9b05380
18. Dutra FR, Silva CS, Custodio R (2021) On the accuracy of the direct method to calculate p*K*a from electronic structure calculations. J Phys Chem A 125:65–73. https://doi.org/10.1021/acs.jpca.0c08283
19. de Souza Silva C. Heats of formation for aluminium compounds with EnAt1 and EnAt2. Theor. Chem. Acc. 139 (2020) https://doi.org/10.1007/s00214-020-02642-8
20. Grimme S (2006) Semiempirical hybrid density functional with perturbative second-order correlation. J Chem Phys 124:034108. https://doi.org/10.1063/1.2148954

21. Boese AD, Martin JML (2004) Development of density functionals for thermochemical kinetics. J Chem Phys 121:3405–3416. https://doi.org/10.1063/1.1774975
22. Zhao Y, Truhlar DG (2008) The M06 suite of density functionals for main group thermochemistry, thermochemical kinetics, noncovalent interactions, excited states, and transition elements: Two new functionals and systematic testing of four M06-class functionals and 12 other function. Theor Chem Acc 120:215–241. https://doi.org/10.1007/s00214-007-0310-x
23. Heyd J, Scuseria GE, Ernzerhof M (2003) Hybrid functionals based on a screened Coulomb potential. J Chem Phys 118:8207–8215. https://doi.org/10.1063/1.1564060
24. Vydrov OA, Scuseria GE (2006) Assessment of a long-range corrected hybrid functional. J Chem Phys 125:234109. https://doi.org/10.1063/1.2409292
25. Adamo C, Barone V (1999) Toward reliable density functional methods without adjustable parameters: the PBE0 model. J Chem Phys 110:6158–6170. https://doi.org/10.1063/1.478522
26. Chai J-Da, Head-Gordon M (2008) Long-range corrected hybrid density functionals with damped atom-atom dispersion corrections. Phys Chem Chem Phys 10:6615–6620. https://doi.org/10.1039/b810189b
27. Cohen AJ, Handy NC (2001) Dynamic correlation. Mol Phys 99:607–615. https://doi.org/10.1080/00268970010023435
28. Adamo C, Barone V (1998) Exchange functionals with improved long-range behavior and adiabatic connection methods without adjustable parameters: The mPW and mPW1PW models. J Chem Phys 108:664–675. https://doi.org/10.1063/1.475428
29. McLean AD, Chandler GS (1980) Contracted Gaussian basis sets for molecular calculations. I. Second row atoms, Z=11–18. J Chem Phys 72:5639–5648. https://doi.org/10.1063/1.438980
30. Krishnan R, Binkley JS, Seeger R, Pople JA. Self-consistent molecular orbital methods. XX. A basis set for correlated wave functions. J Chem Phys 72 (1980) 650–654. https://doi.org/10.1063/1.438955
31. Dunning TH (1989) Gaussian basis sets for use in correlated molecular calculations. I. The atoms boron through neon and hydrogen. J Chem Phys 90:1007–1023. https://doi.org/10.1063/1.456153
32. Kendall RA, Dunning TH, Harrison RJ (1992) Electron affinities of the first-row atoms revisited. Systematic basis sets and wave functions. J Chem Phys 96:6796–6806. https://doi.org/10.1063/1.462569
33. Baboul AG, Curtiss LA, Redfern PC, Raghavachari K (1999) Gaussian-3 theory using density functional geometries and zero-point energies. J Chem Phys 110:7650–7657. https://doi.org/10.1063/1.478676
34. Wood GPF, Radom L, Petersson GA, et al (2006) A restricted-open-shell complete-basis-set model chemistry. J Chem Phys 125. https://doi.org/10.1063/1.2335438
35. Chinini GL, Custodio R (2019) Assessment of a composite method based on selected density functional theory methods and complete basis set extrapolation formulas. Int J Quantum Chem 119:1–12. https://doi.org/10.1002/qua.25892
36. Frisch MJ, Trucks GW, Schlegel HB, et al (2016) Gaussian 09, Revision A.02, Gaussian, Inc., Wallingford, CT
37. Caldeira MT, Custodio R (2019) Partial combination of composite strategy and the B3LYP functional for the calculation of enthalpies of formation. J Mol Model 25. https://doi.org/10.1007/s00894-019-3952-4
38. Lu L (2015) Can B3LYP be improved by optimization of the proportions of exchange and correlation functionals? Int J Quantum Chem 115:502–509. https://doi.org/10.1002/qua.24876
39. NIST Chemistry Webbook. http://webbook.nist.gov/chemistry
40. Karton AM, Martin JML (2007) Heats of formation of beryllium, boron, aluminum, and silicon re-examined by means of W4 theory J Chem Phys 111. https://doi.org/10.1021/jp071690x
41. Snyder LC, Basch H (1969) Heats of reaction from self-consistent field energies of closed-shell molecules, J Am Chem Soc 91. https://doi.org/10.1021/ja01037a001.
42. Hehre WJ , Ditchfield R, Radom L, Pople JA (1970) Molecular orbital theory of the electronic structure of organic compounds. V. Molecular theory of bond separation. J Am Chem Soc 92
43. Ditchfield R, Hehre WJ, Pople JA, Radom L (1970) Molecular orbital theory of bond separation. Chem Phys Lett 5. https://doi.org/10.1016/0009-2614(70)80116-6.